

Lightweight photophoretic flyers with germanium coatings as selective absorbers

Zhipeng Lu,¹ Gulzhan Aldan¹,² Danielle Levin¹,² Matthew F. Campbell¹,² and Igor Bargatin¹,^{2,*}

¹*Department of Chemistry, University of Pennsylvania, Philadelphia, Pennsylvania, USA*

²*Department of Mechanical Engineering and Applied Mechanics, University of Pennsylvania, Philadelphia, Pennsylvania, USA*

(Received 8 June 2023; revised 5 January 2024; accepted 18 March 2024; published 9 April 2024)

The goal of ultrathin lightweight photophoretic flyers, or light flyers for short, is to levitate continuously in Earth's upper atmosphere using only sunlight for propulsive power. We previously reported light flyers that levitated by utilizing differences in thermal accommodation coefficient between the top and bottom of a thin film, made possible by coating their lower surfaces with carbon nanotubes (CNTs). Such designs, though successful, had relatively high thermal emissivity (>0.5), which prevented them from achieving high temperatures and resulted in their transferring relatively low amounts of momentum to the surrounding gas. To address this issue, we have developed light flyers with ultrathin undoped germanium layers that selectively absorb nearly 80% of visible light but are mostly transparent in the thermal infrared, with an average thermal emissivity of <0.1 . Our experiments show that germanium-coated light flyers could levitate at up to 43% lower light irradiances than mylar-CNT disks with identical sizes. In addition, we simulated our experiments using a semiempirical model, which allowed us to predict that our 2-cm-diameter disk-shaped germanium-coated light flyers can levitate in the mesosphere (altitudes 67–75 km) under the natural sunlight (1.36 kW/m^2). Similar ultrathin selective-absorber coatings can also be applied to three-dimensional light flyers shaped like solar balloons, allowing them to carry significant payloads and thereby revolutionize long-term atmospheric exploration of Earth or Mars.

DOI: 10.1103/PhysRevApplied.21.044019

Unmanned aerial vehicles (UAVs) can potentially carry out extensive, long-lasting, and cost-effective exploration of Earth's atmosphere. One proposed kind of small UAVs—sunlight-powered photophoretic flyers, or light flyers—can levitate in midair using a temperature gradient across a nanocardboard plate [1,2] or by taking advantage of a difference in the thermal accommodation coefficient (TAC) between two sides of a thin film [3].

Previously reported light flyers have not yet been suitable for deployment in Earth's upper atmosphere or on Mars because they required irradiance levels many times that of natural sunlight. The natural sunlight irradiance is 1.36 kW/m^2 under normal incidence in the mesosphere or stratosphere, approximately 1 kW/m^2 at sea level on Earth, and $<0.6 \text{ kW/m}^2$ on Mars. In contrast, we previously reported levitation of 6-mm-diameter mylar-carbon-nanotube (CNT) disks at irradiances above 5 kW/m^2 [3] and 8-mm-wide nanocardboard plates at irradiances above 10 kW/m^2 [1], with both observed at room temperature in a vacuum chamber.

Recent theoretical studies suggest the possibility of not just levitation, but also carrying significant payloads in

Earth's upper atmosphere, where the ambient temperatures are much lower than at sea level. For instance, Schafer *et al.* [2] predicted that a 10-cm-diameter disk using alumina-based nanocardboard composites could carry a 0.3-g payload in the stratosphere, roughly 10 times the craft's mass and sufficient for simple silicon-based sensors. Additionally, Celenza *et al.* [4] simulated three-dimensional (3D) meter-scale porous structures capable of carrying much larger kilogram-scale payloads in the upper mesosphere [see Fig. 1(b)]. Though holding significant promise, these results have yet to be practically demonstrated. Laboratory experiments are therefore crucial to confirm the lift forces generated by thermal transpiration or Knudsen pump mechanisms and to move toward real-world applications of these light flyers.

All other things being equal, the photophoretic force increases with decreasing thermal emissivity, because this typically causes the light flyer to be hotter relative to the ambient atmosphere. Similarly, increasing TAC difference between the two surfaces is also beneficial because this results in a greater momentum differential between gas molecules colliding with the top and bottom surfaces [3]. Since all TAC values in air are fairly close to unity due to a molecularly thin organic layer spontaneously formed under ambient conditions [6], it is difficult to increase

*bargatin@seas.upenn.edu, bargatin@gmail.com

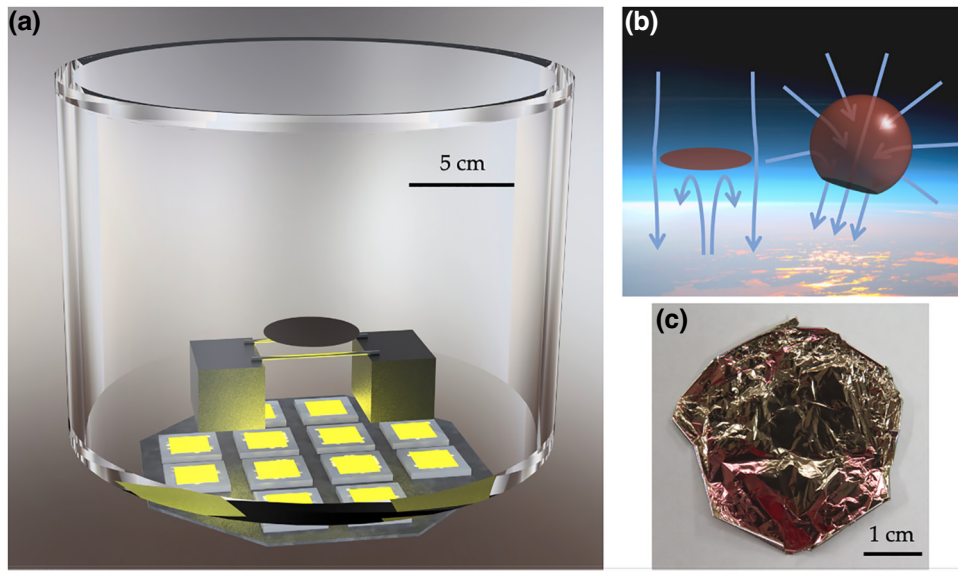


FIG. 1. (a) Schematic diagram of the experimental setup consisting of an acrylic vacuum chamber, a 4-cm-diameter germanium-coated light flyer, two 2.4-mm-diameter aluminum rods on two 4.5-cm-tall substrates, and 12 LEDs below the chamber. (b) Conceptual diagram of a germanium-coated light-flyer disk (left) and solar-photophoretic balloon (right) in the mesosphere. The background is courtesy of NASA [5]. (c) Photograph of a 4-cm-diameter alumina-germanium-myler-germanium light flyer. We observed that the spontaneous wrinkling of this light flyer helped to maintain its flat shape during levitation.

the difference in TAC beyond 10%–20% even for clean well-characterized surfaces [7,8]. However, it is possible to create light flyers with very low thermal emissivity values by coating them with a selective absorber that has a high absorptivity for the solar spectrum but low emissivity in the thermal infrared (5–15- μm wavelength). Many semiconductors possess such optical properties as long as their band gaps fall at energies between those of the visible and thermal infrared spectra (i.e., 0.35–1.4 eV [9]). Among these options, undoped germanium is easy to deposit, is nearly transparent in the thermal infrared spectrum [10], and thus has very low emissivity, making it an ideal candidate for our selective absorber.

As detailed in the following, our use of germanium resulted in a significant reduction in the light irradiance needed for levitation from 2.5 kW/m^2 for CNT-coated light flyers to just 1.5 kW/m^2 for germanium-coated flyers. To corroborate our findings, we also measured the optical and surface properties of germanium and developed a theoretical model to predict the light flyer's levitating performance in both the laboratory and in Earth's mesosphere. Importantly, our model predicts that natural sunlight (approximately 1 kW/m^2) would be sufficient for levitation in the mesosphere because the ambient temperatures there are much lower than in our laboratory experiments.

We fabricated disk-shaped light flyers by sputtering germanium as the light-absorbing layer on both sides of a 500-nm-thick mylar film, then atomic-layer-depositing (ALD) a 50-nm-thick layer of alumina onto one side of the film to enhance the light flyer's mechanical and

thermal robustness (see Supplemental Material [11] for details). Depositing alumina on both sides creates a symmetric structure resulting in no significant TAC difference between the top and bottom sides. Hence, for the purpose of this study, only one side of the film has the alumina. In the final stage of the fabrication process, we laser-cut circular disks of different sizes from our germanium-mylar-germanium-alumina films. Figure 1(c) shows a representative germanium-coated disk, where the spontaneous wrinkling of the surfaces resulted from the inherent nonuniform stresses in the mylar film. This feature increased the thermal resilience since, in our experience, wrinkled samples bent and curved less than planar samples under intense light.

We tested our light flyers in a cylindrical acrylic vacuum chamber and illuminated them from below using an arrangement of twelve 100-W light-emitting diode (LED) arrays, which created irradiances of up to 6 kW/m^2 (6 Suns). In a single experiment, we held the chamber pressure constant while gradually increasing the light irradiance until the light flyer lifted off; we then repeated this procedure at different pressures. Notice that the LED light generally came from below the light flyer, in contrast to the real-world deployment in the mesosphere where sunlight shines from above. However, we have previously determined that the photophoretic force is independent of the direction of the incoming light, since the top side of the light flyer is transparent and the light is always absorbed in the germanium layer on the bottom side.

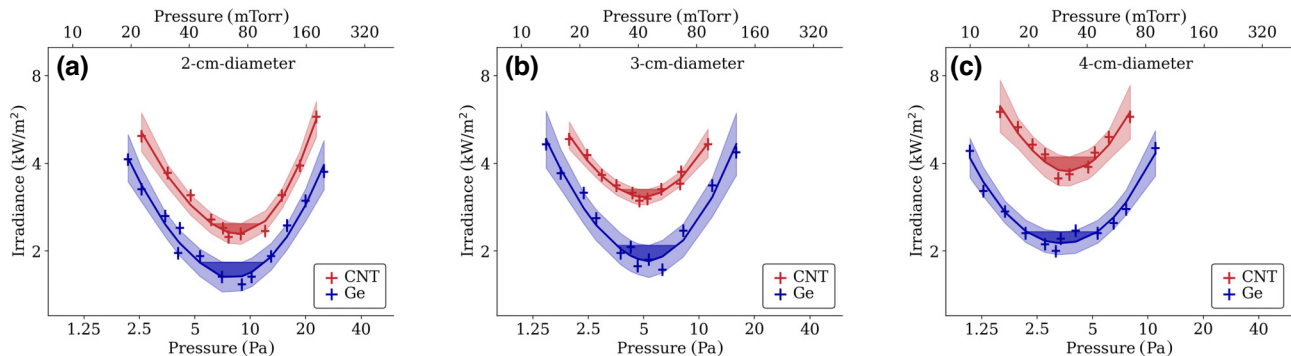


FIG. 2. Levitation performance of alumina-mylar disks with Ge or carbon nanotube (CNT) absorber coatings and diameters of (a) 2, (b) 3, and (c) 4 cm. The flyers were launched from two aluminum rods (2.4 mm in diameter) that were placed far from the vacuum chamber's bottom (4.5 cm). Solid lines show locally estimated scatterplot smoothing fits, with 99% confidence intervals marked with light shading. Estimated optimal pressures and minimum irradiances are shown with darker shading.

Vacuum chamber levitation experiments can be impacted by the ground effect, in which an enhanced lift force is generated when the light flyer is close to the chamber floor [15]. To avoid overestimating the lift force due to this effect, we followed the guidelines from Ref. [15] for minimizing the launchpad-associated ground effect. This involved using a sparse launchpad consisting of two 2.4-mm-diameter aluminum rods, as shown in Fig. 1(a). These thin aluminum rods exhibited a minimal ground effect similar to that of the J-shaped steel wires from Ref. [11], as shown in the Supplemental Material Fig. S2. We used the rods rather than the wires because they were more convenient in sample loading and testing. We also positioned the launchpad about 4.5 cm above the chamber floor, a distance greater than the diameter of the largest sample, in order to minimize the floor-associated ground effect [11].

Figure 2 illustrates the impact of the selective-absorption coating by comparing the levitation of germanium-coated light flyers to those with previously reported CNT-coatings [3,15]. It can be seen that, for all disk sizes, the irradiance required for levitation was lower for Ge-coated light flyers, demonstrating the impact of this type of coating. Specifically, the minimum irradiances needed for levitation were 29%, 39%, and 43% lower for 2-, 3-, and 4-cm-diameter germanium light flyers, respectively. The significant decrease can be attributed to the much lower emissivity of germanium, which increases the temperature of germanium-coated samples compared to CNT-coated ones. Specifically, for the 2-cm-diameter disks under the optimal pressure (around 7 Pa) and 1.5 kW/m² incident irradiance, our model (discussed later) predicts a 450 K temperature for the germanium-coated samples at its optimal pressure, whereas that for the CNT-coated samples is 385 K. This discrepancy in the surface temperature suggests that a greater reduction in germanium's emissivity (up to 80%, as discussed later) offsets the slight reduction in its TAC (only 10% difference, as discussed later, compared to the CNT's 25%). Larger

disks exhibited greater reductions in minimum irradiances due to their higher surface area and thus higher importance of radiative heat dissipation and lower relative importance of air conduction. Mathematical details of the emissivity's effect on the disk temperature and photophoretic force are described in the Supplemental Material [11].

Plotting the minimum irradiance needed for levitation versus the chamber pressure shows a parabola-like minimum in the log-log scale (Fig. 2). The photophoretic force was both predicted [16–18] and observed [15] to reach a maximum at pressures where the mean free path is proportional to the disk diameter (i.e., for $\text{Kn} \sim 0.047$, where Kn is the Knudsen number, equal to the ratio of the gas's mean free path to the diameter of the levitating disk). The bottom of the parabola corresponds to the *optimal pressure* that maximizes the lift force.

We extensively characterized our films in order to better understand their optical and thermal accommodation properties. Our experiments included measuring the optical properties of our films using both thermal imaging and transmittance-only Fourier-transform infrared (FTIR) spectrometry to test our hypothesis that germanium leads to a lower emissivity than CNTs. We note that precise measurements of the material's optical properties require rigorous analysis and a system consisting of the radiation source, sample, and detector. The ideal way to do this is to use a home-built FTIR spectrometer method with an emission measurement attachment [19], but rough estimates can be done via thermal imaging and transmittance-only FTIR spectrometry as detailed in the following. We also measured the films' TAC values using a concentric spherical-shell configuration [7] and their roughness using atomic force microscopy (AFM).

The ability of materials to lose heat by radiation is characterized by their emissivity (ε), which is related to their transmittance (t) and reflectance (r) at the same wavelength through the equation $\varepsilon = 1 - t - r$. First, we estimated the transmittance and reflectance at thermal

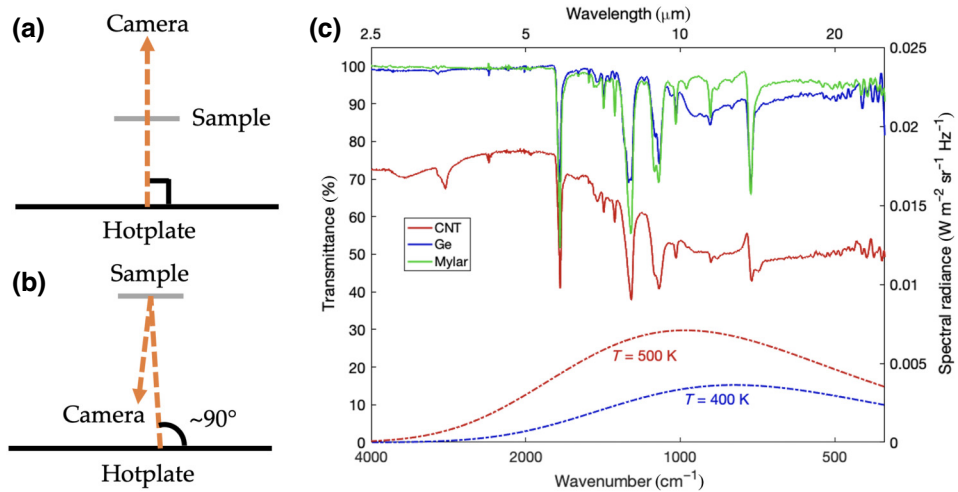


FIG. 3. Characterization results of optical properties from (a),(b) thermal imaging and (c) transmittance-only FTIR. Schematics of the thermal imaging method measuring the 90° (a) transmittance and (b) reflectance. (c) The left axis plots the transmittance of various films as characterized by FTIR, while the right plots the calculated spectral radiance of black body radiation at 400 and 500 K surface temperature. The shaded area highlights the spectrum where transmittance is averaged.

infrared wavelengths using thermal imaging. To conduct this test, as shown in Figs. 3(a) and 3(b), we used a hotplate as a radiation source and measured thermal infrared radiation transmitted and reflected by a light-flyer film at normal incidence using a thermal camera. The details are described in the Supplemental Material [11]. Subtracting 90° transmittance and reflectance from unity resulted in the emissivities of approximately 0.08 and 0.48 for germanium and CNT-based films, respectively, as tabulated in Table I. Using a similar measurement in the optical frequency range, we also estimated the visible-range absorptivity of both CNT and germanium to be 0.75 using a white flashlight as the light source. It is highlighted that the optical data for mylar-alumina films are not listed in Table I because their optical properties vary little from bare mylar films and hence are of low interest.

As shown in Fig. 3(c), we also measured the transmittance of mylar, mylar-CNT, and mylar-germanium light-flyer materials at wavenumbers from 4000 to 400 cm^{-1} using a FTIR spectrometer. To estimate an upper bound for emissivity, we assumed zero reflectance of the films, giving the upper bound $\varepsilon_{\max} = 1 - t$. Based on the expected

temperatures of 400 to 500 K for a light flyer under sunlight, spectral emission reaches a maximum at approximately 900 cm^{-1} , corresponding to a wavelength of $11 \mu\text{m}$. Therefore, by averaging the transmittance in the range $900 \pm 400 \text{ cm}^{-1}$, where the black body radiation peaks at temperatures between 400 and 500 K, we derived the upper bounds for emissivity to be 0.11 and 0.49 for germanium and CNT-based films, respectively, values that agree with those obtained through thermal imaging. Our results show that germanium has nearly 5 times lower emissivity than CNTs, resulting in significantly larger temperatures and a stronger photophoretic lift force.

Next, we characterized the TAC values of various surfaces using the experimental setup described in Ref. [7]. We first calibrated our experimental setup by comparing results of gold and platinum with literature values. We then prepared the same samples as for FTIR spectrometry and averaged three sets of results for each of mylar, mylar-germanium, and mylar-CNT, as tabulated in Table I, as well as mylar-alumina. Specifically, mylar-alumina had a TAC of 0.79 ± 0.03 . The measured TAC values between 0.8 and 1.1 in air are consistent with literature reports that the TAC is usually close to unity for interactions with relatively heavy molecules, such as nitrogen and oxygen [7,8,20]. We note that, although the TAC is defined to be between 0 and 1, the measured TAC may be slightly larger than unity due to systematic measurement errors [21,22]. However, the differences between the TACs of any two materials, which is the quantity needed to predict photophoretic forces, are accurate even in the presence of such systematic errors. Our measurements, summarized in Table I, show that the typical TAC difference between a top layer (e.g., mylar or alumina) and a bottom one (i.e.,

TABLE I. Optical properties and TAC for various materials.

Property	Mylar	Mylar-Ge	Mylar-CNT
IR transmittance	0.92 ± 0.01	0.81 ± 0.01	0.47 ± 0.02
IR reflectance	0.02 ± 0.01	0.11 ± 0.01	0.05 ± 0.01
IR emissivity	0.06 ± 0.02	0.08 ± 0.02	0.48 ± 0.03
Visible transmittance	0.94 ± 0.01	0.18 ± 0.01	0.22 ± 0.01
Visible reflectance	0.02 ± 0.01	0.07 ± 0.02	0.03 ± 0.01
Visible absorptivity	0.03 ± 0.02	0.75 ± 0.03	0.75 ± 0.02
TAC	0.77 ± 0.03	0.90 ± 0.03	1.08 ± 0.05

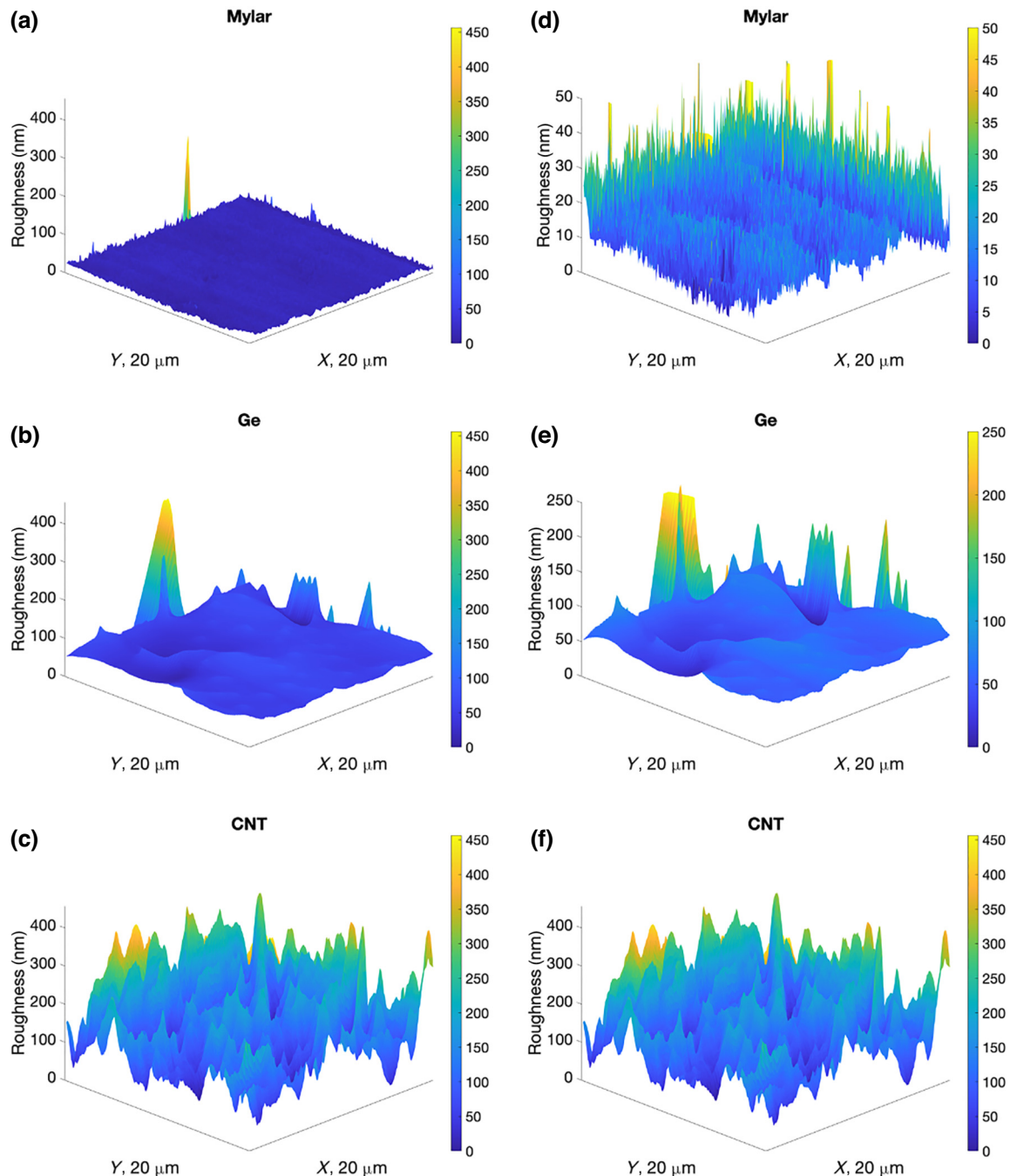


FIG. 4. Characterization results of surface properties from atomic force microscopy. (a)–(c) Three-dimensional surface roughness graphs focusing on $20 \times 20 \mu\text{m}^2$ spots for (a) mylar, (b) mylar-Ge, and (c) mylar-CNT surfaces. (d)–(f) Rescaled graphs to exclude friction enhancement particles.

germanium or CNT) is approximately 0.1 for germanium-based light flyers and 0.25 for CNT-based ones. Details are described in the Supplemental Material [11].

Surface roughness is one of the factors affecting the TAC, with greater roughness typically resulting in a higher TAC because an incident molecule is more likely to collide multiple times with a rough surface and therefore reach a higher degree of thermalization. To better understand

our TAC findings, we conducted AFM on various surfaces we used for light flyers. As shown in Figs. 4(b)–4(d), the root-mean-squared (rms) roughness of mylar, mylar-germanium, and mylar-CNT were 2.5, 34.8, 71.2 nm, respectively. This upward trend aligns well with the TAC values presented in Table I, where smoother surfaces have a lower rms roughness and consequently lower TAC. Note that tall (100–400 nm) peaks observed in Figs. 4(a) and

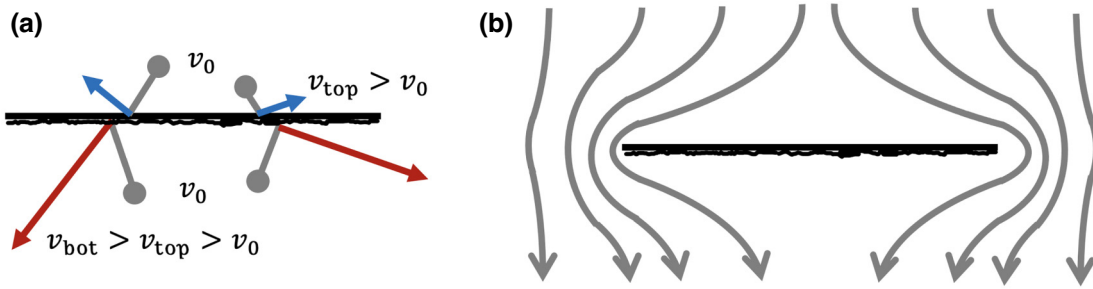


FIG. 5. Schematics of photophoretic forces in (a) free-molecular and (b) continuum regimes. v_0 denotes the initial velocities of gas molecules before colliding with the surface, while v_{top} and v_{bot} represent the velocities of gas molecules after colliding with the top and bottom surfaces, respectively.

4(b) are associated with submicron particles intentionally included in the mylar sheet by the manufacturer to reduce stiction. These rare inclusions do not affect the number of collisions between a molecule and the surface and therefore were not included in the rms roughness comparison. Environmental scanning electron microscopy images of these particles on both mylar and mylar-germanium surfaces are shown in the Supplemental Material Fig. S4 [11].

Despite their lower TAC difference, the much lower emissivity of germanium-coated light flyers still offers net advantages in real-world levitation applications in Earth's mesosphere or on Mars. It is therefore important to conduct experiments in a low-temperature vacuum chamber at the conditions of the mesosphere. While

state-of-the-art techniques can cool down the vacuum chamber by approximately 100 K using dry ice or other vacuum cooling methods [23,24], these techniques are expensive and challenging to implement, especially under high optical flux. Instead, we performed experiments at room temperature and used them to develop a revised model for our light flyers based on the photophoresis theory and our experimental data.

According to Rohatschek's work [17], the semiempirical equation of the photophoretic force is $1/F = 1/(C_{\text{FM}}F_{\text{FM}}) + 1/(C_{\text{cont}}F_{\text{cont}})$, where F stands for the photophoretic force, subscripts FM and cont for free-molecular and continuum regime, respectively, and C_{FM} and C_{cont} are typically assumed to be 1 for atmospheric aerosols [17,25]. In the free-molecular regime where the ambient pressure

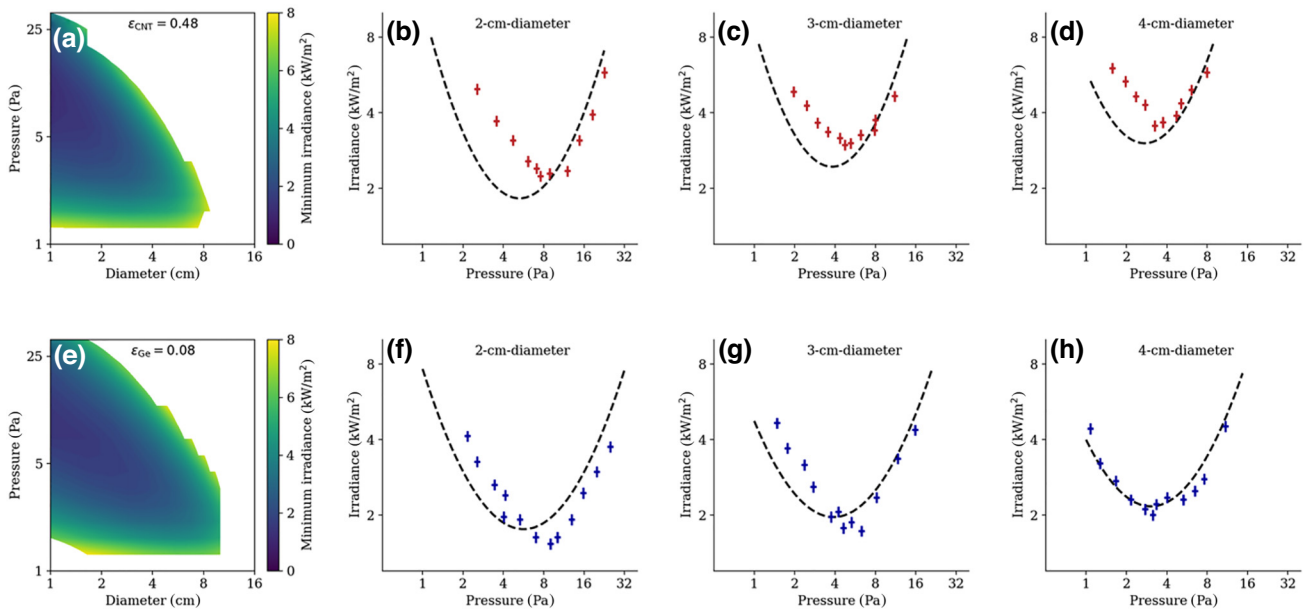


FIG. 6. Theoretical predictions and experimental data. Contour maps of the minimum irradiance for (a) CNT-coated disks (by assuming a uniform emissivity $\varepsilon_{\text{CNT}} = 0.48$) and (e) germanium-coated disks (by assuming $\varepsilon_{\text{Ge}} = 0.08$). Predicted irradiance-pressure curves and the experimental irradiance-pressure data for (b)–(d) CNT-coated disks and (f)–(h) germanium-coated disks with diameters of (b),(f) 2, (c),(g) 3, and (d),(h) 4 cm.

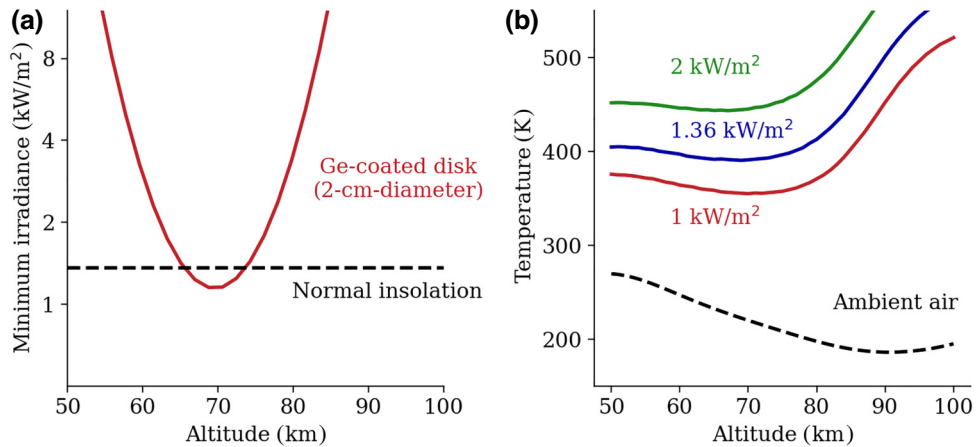


FIG. 7. Key predictions from the theoretical model. All plots assume a germanium-coated light flyer with top TAC $\alpha_{\text{top}} = 0.9$, bottom TAC $\alpha_{\text{bot}} = 0.8$, uniform emissivity $\varepsilon = 0.08$, optical absorptivity $\epsilon_{\text{vis}} = 0.75$, and areal density $\rho = 1.0 \text{ g/m}^2$. (a) The minimum irradiance required for a 2-cm-diameter light flyer vs altitude. The black dashed line stands for the normal solar insolation (i.e., 1.36 kW/m^2). (b) The temperature profiles of this 2-cm-diameter light flyer at different irradiance levels and the ambient air vs altitude.

is low, the momentum difference in gas molecules colliding with the top and bottom surfaces exerts an upward force pointing from the high-TAC to low-TAC side. In the continuum regime where the ambient pressure is high, the thermal creep flow around the sample creates the reaction force in the same direction (pointing from the high-TAC to low-TAC side). For a sphere with no discontinuous boundaries, the main approximations used by Rohatschek were about the value of the thermal creep coefficient and the use of interpolation $1/F = 1/F_{\text{FM}} + 1/F_{\text{cont}}$. In our case, we took the limit of an oblate spheroid to approach the flat-disk light flyer.

However, the case of $C_{\text{FM}} = C_{\text{cont}} = 1$, valid for spherical microparticles, did not agree with our experimental observations of ultrathin disks. Instead, as shown in Fig. 6, $C_{\text{fm}} = 0.19$ and $C_{\text{cont}} = 2$ fitted our experimental observations at all pressures for all light-flyer sizes of both germanium and CNT-coated samples. Our use of C_{FM} and C_{cont} as fitting parameters is motivated by the recognition that the original semiempirical interpolation method is most accurate in either free-molecular or continuum regimes and is least accurate in the transition regime. However, the TAC-difference-photophoretic force reaches its maximum in the transition regime where the physics involved is complex, which necessitates adjustments to these two coefficients. When dealing with significantly lower or higher pressures, $C_{\text{FM}} = C_{\text{cont}} = 1$ remains valid. Nevertheless, fitting is necessary in the transitional flow region before an accurate and comprehensive model can be developed specifically for the transition regime, which is most useful in practical applications. Specific equations for the derivation of the light flyer's temperature and

photophoretic force are discussed in the Supplemental Material [11].

This theoretical model of the light flyer's performance in our laboratory vacuum chamber can be applied to Earth's mesosphere as well. Earth's mesosphere extends from 50 to 100 km in altitude [26,27], with pressures ranging from 75 to 0.025 Pa (i.e., 560 to 0.19 mTorr). The ambient temperature in the mesosphere varies between 180 and 270 K, significantly lower than the room temperature in our vacuum chamber (293 K). The high-altitude temperature profile therefore offers considerable room for performance improvements, such as more effective radiative heat dissipation and less thermal deformation of mylar.

Next, we considered the 2-cm-diameter germanium-coated light flyer as an example since it had a lower minimum irradiance than the 3- and 4-cm-diameter disks. As shown in Fig. 7(a), assuming a normal solar insolation of 1.36 kW/m^2 on top of Earth's atmosphere [28,29], this light flyer could levitate at an altitude of between 67 and 75 km, corresponding to a pressure range of 7.4 to 2.1 Pa (i.e., 56 to 16 mTorr). A more conservative estimate can be considered by assuming an incident angle of the sunlight smaller than 90° , which would be typical for a light flyer without any tilting mechanism [2]. Even at a 45° incident angle, the insolation would still be nearly 1.0 kW/m^2 , narrowing the altitude range slightly to 69–73 km. Fig. 7(b) demonstrates the temperatures of the light flyer at different solar irradiance levels of 1, 1.36, and 2 kW/m^2 , corresponding to solar incident angles of 45° , normal, and normal plus sunlight reflected due to ground albedo. Importantly, the temperatures remain significantly below the thermal deformation temperature of mylar,

which is around 500 K. Hence, these results suggest that a long-lasting levitation in a 4-km-wide altitude range may be possible, despite strong wind shears in the mesosphere [29,30]. The outcomes for 3- and 4-cm-diameter disks are presented in Fig. S7 of Supplemental Material [11], indicating a gradual reduction in the operational pressure and altitude range (Fig. 7).

Maximum payloads can also be derived from the model, as discussed in the Supplemental Material [11]. For light-flyer disks a few centimeters in diameter, the payload is generally in the milligram range, which is challenging for practical applications. Similar (milligram range) payloads were predicted in Ref. [7], but those predictions assumed hypothetical values of emissivity and thermal accommodation coefficient. Our predictions in the paper are fully based on experimentally measured properties. Moreover, Celenza *et al.* recently showed that 3D structures made from nanocardboard can increase the payload to the kilogram range [4]. Using germanium as a light-absorbing coating in these structures would greatly increase (approximately double) the photophoretic force by reducing the thermal emissivity.

In summary, we have demonstrated light flyers composed of alumina and mylar as structural layers and germanium as a selective absorber. Unlike most commonly used ceramic-metal selective absorbers [31], which are relatively thick and heavy and have low emissivity because they are highly reflective in the thermal infrared, our ultra-thin germanium layer is highly transparent in the thermal infrared range. We conducted tests on germanium-coated disks with diameters of 2, 3, and 4 cm under minimized ground-effect conditions and achieved successful levitations at irradiance levels as low as 1.5 kW/m^2 at room temperature. We characterized the optical and surface properties of germanium and CNT-based films and found germanium to have a sixfold lower emissivity. Using experimental data and a semiempirical photophoretic force, we developed a revised model and predicted levitation capabilities at various altitudes for light flyers of multiple sizes. In addition to the two-dimensional photophoretic light-flyer disks, the germanium coating can be applied on 3D geometries like the balloon designs of Celenza *et al.* [4] to reduce radiative heat loss and increase the photophoretic force, paving the way for future low-cost and clean-energy atmospheric research.

-
- [1] J. Cortes, C. Stanczak, M. Azadi, M. Narula, S. M. Nicaise, H. Hu, and I. Bargatin, Photophoretic levitation of macroscopic nanocardboard plates, *Adv. Mater.* **32**, 1906878 (2020).
- [2] B. C. Schafer, J. Kim, J. J. Vlassak, and D. W. Keith, Analytical models for the design of photophoretically levitating macroscopic sensors in the stratosphere, *ArXiv:2209.08093* (2022).
- [3] M. Azadi, G. A. Popov, Z. Lu, A. G. Eskenazi, A. J. W. Bang, M. F. Campbell, H. Hu, and I. Bargatin, Controlled levitation of nanostructured thin films for sun-powered near-space flight, *Sci. Adv.* **7**, eabe1127 (2021).
- [4] T. Celenza, A. Eskenazi, and I. Bargatin, 3D photophoretic aircraft made from ultralight porous materials can carry kg-scale payloads in the mesosphere, *ArXiv:2301.04281* (2023).
- [5] National Aeronautics and Space Administration, SOFIA Offers New Way to Study Earth's Atmosphere, <https://www.nasa.gov/missions/station/sofia-offers-new-way-to-study-earths-atmosphere/> (2021).
- [6] C. D. F. Honig and W. A. Ducker, Effect of molecularly-thin films on lubrication forces and accommodation coefficients in air, *J. Phys. Chem. C* **114**, 20114 (2010).
- [7] H. Yamaguchi, T. Imai, T. Iwai, A. Kondo, Y. Matsuda, and T. Niimi, Measurement of thermal accommodation coefficients using a simplified system in a concentric sphere shells configuration, *J. Vac. Sci. Technol., A* **32**, 6 (2014).
- [8] D. J. Rader, J. N. Castaneda, J. R. Torczynski, T. W. Grasser, and W. M. Trott, *Measurements of Thermal Accommodation Coefficients (No. SAND2005-6084)* (Sandia National Laboratories (SNL), Albuquerque, NM, and Livermore, CA, 2005).
- [9] F. Zhuge, Z. Zheng, P. Luo, L. Lv, Y. Huang, H. Li, and T. Zhai, Nanostructured materials and architectures for advanced infrared photodetection, *Adv. Mater. Technol.* **2**, 8 (2017).
- [10] E. Takasuka, E. Tokizaki, K. Terashima, and S. Kimura, Emissivity of liquid germanium in visible and near infrared region, *J. Appl. Phys.* **82**, 2590 (1997).
- [11] See Supplemental Material at <http://link.aps.org-supplemental/10.1103/PhysRevApplied.21.044019> for the details on the vacuum chamber and LED setup; launchpad selection; levitation performance of another set of light flyers; light-flyer fabrication procedure and characterization; TAC measurement and data processing; theoretical modeling for light flyers; and prediction of light flyers for mesospheric applications. The Supplemental Material also contains Refs. [12–14].
- [12] W. M. Trott, D. J. Rader, J. N. Castañeda, J. R. Torczynski, M. A. Gallis, and T. Abe, Measurement of gas-surface accommodation, measurement of gas-surface accommodation, *AIP Conf. Proc.* **1084**, 621 (2008).
- [13] U.S. Standard Atmosphere vs. Altitude, https://www.engineeringtoolbox.com/standard-atmosphere-d_604.html (n.d.).
- [14] R. Carmichael, A Table of the Standard Atmosphere to 86 km in SI Units, <https://www.pdas.com/atmosTable1SI.html> (2021).
- [15] Z. Lu, M. Stern, J. Li, D. Candia, L. Yao-Bate, T. J. Celenza, M. Azadi, M. F. Campbell, and I. Bargatin, Minimizing the ground effect for photophoretically levitating disks, *Phys. Rev. Appl.* **19**, 044004 (2023).
- [16] H. Rohatschek, Photophoresis and accommodation, *Оптика Атмосферы и Океана* **27**, 87 (2014).
- [17] H. Rohatschek, Semi-empirical model of photophoretic forces for the entire range of pressures, *J. Aerosol Sci.* **26**, 717 (1995).
- [18] N. T. Tong, Photophoretic force in the free molecule and transition regimes, *J. Colloid Interface Sci.* **43**, 78 (1973).

- [19] K. Mizuno, J. Ishii, H. Kishida, Y. Hayamizu, S. Yasuda, D. N. Futaba, M. Yumura, and K. Hata, A black body absorber from vertically aligned single-walled carbon nanotubes, *Proc. Natl. Acad. Sci. U. S. A.* **106**, 6044 (2009).
- [20] W. M. Trott, J. N. Castañeda, J. R. Torczynski, M. A. Gallis, and D. J. Rader, An experimental assembly for precise measurement of thermal accommodation coefficients, *Rev. Sci. Instrum.* **82**, 3 (2011).
- [21] W. Trott, D. Rader, J. Castaneda, J. Torczynski, and M. Gallis, in *39th AIAA Thermophysics Conference* (2007), pp. 4039.
- [22] P. T. C. Chen, R. J. Hedgeland, and S. R. Thomson, in *Optical System Contamination: Effects, Measurement, Control II* (1990), pp. 1329.
- [23] W. Burgmann and K. Göhler, Modern vacuum pumps for the vacuum degassing of steel in small and large vacuum-degassing units, *Metallurgist* **57**, 516 (2013).
- [24] S. Thiangchanta, T. A. Do, W. Tachajapong, and Y. Mona, Experimental investigation of the thermoelectric cooling with vacuum wall system, *Energy Rep.* **6**, 1244 (2020).
- [25] U. von Zahn, J. Höffner, V. Eska, and M. Alpers, The mesopause altitude: Only two distinctive levels worldwide?, *Geophys. Res. Lett.* **23**, 3231 (1996).
- [26] H. Rohatschek, Direction, magnitude and causes of photophoretic forces, *J. Aerosol Sci.* **16**, 29 (1985).
- [27] M. Venkat Ratnam, A. K. Patra, and B. V. Krishna Murthy, Tropical mesopause: Is it always close to 100 km?, *J. Geophys. Res.: Atmos.* **115**, D06106 (2010).
- [28] O. Coddington, J. L. Lean, P. Pilewskie, M. Snow, and D. Lindholm, A solar irradiance climate data record, *Bull. Am. Meteorol. Soc.* **97**, 1265 (2016).
- [29] L. Qian, C. Jacobi, and J. McInerney, Trends and solar irradiance effects in the mesosphere, *J. Geophys. Res. Space Phys.* **124**, 1343 (2019).
- [30] A. Müllermann and F.-J. Lübken, Horizontal winds in the mesosphere at high latitudes, *Adv. Space Res.* **35**, 1890 (2005).
- [31] C. E. Kennedy, *Review of Mid-to High-Temperature Solar Selective Absorber Materials* (No. NREL/TP-520-31267) (National Renewable Energy Lab., Golden, CO, USA, 2002).